MATERIALS CHEMISTRY FRONTIERS

CCS 中国化学会 CHINESE CHEMICAL SOCIETY

ICCAS

ROYAL SOCIETY OF CHEMISTRY

Very low lasing threshold of DABNA derivatives with DFB structures

Journal:	*Materials Chemistry Frontiers*
Manuscript ID	QM-RES-10-2022-001040.R1
Article Type:	Research Article
Date Submitted by the Author:	21-Nov-2022
Complete List of Authors:	Mamada, Masashi; Kyushu University, Center for Organic Photonics and Electronics Research (OPERA) Maedera, Satoshi ; Kyushu University, Center for Organic Photonics and Electronics Research (OPERA) Oda, Susumu; Kwansei Gakuin University - Kobe Sanda Campus, Nguyen, Thanh; Kyushu University, Center for Organic Photonics and Electronics Research (OPERA) Nakanotani, Hajime; Kyushu University, Center for Organic Photonics and Electronics Research (OPERA) Hatakeyama, Takuji; Kyoto University, Department of Chemistry Adachi, Chihaya; Kyushu University, Center for Organic Photonics and Electronics Research (OPERA)

ARTICLE

Very low lasing threshold of DABNA derivatives with DFB structures

Received 00th January 20xx,
Accepted 00th January 20xx

DOI: 10.1039/x0xx00000x

Masashi Mamada*[ab], Satoshi Maedera[a], Susumu Oda,[c] Thanh Ba Nguyen[a], Hajime Nakanotani[ab], Takuji Hatakeyama[d], and Chihaya Adachi*[ab]

For elucidating the potential of light amplification properties of thermally activated delayed fluorescence materials (TADF), the distributed feedback (DFB) laser devices using DABNA derivatives having a multiple-resonance effect were fabricated. We demonstrated a very low lasing threshold of 0.27 μJ cm^{-1}, which is the best performance in TADF materials, for 6 wt%-DABNA-2 doped in an mCBP host layer combined with a mixed-order DFB structure. Further, by focusing on the photophysical properties of aggregated states of DABNA derivatives, advanced light amplification architectures composed of dual DABNA derivatives were examined. Consequently, the DABNA-based films also provided remarkably low lasing thresholds in high concentrations.

1. Introduction

Organic lasers have the potential applications to complement inorganic laser technologies, thereby captivating the attention of the photonics and optoelectronics community after the first demonstration of lasing from organic solution in 1966.[1] Since solid-state lasers are highly attractive in terms of low cost, light in weight, and compact, recent efforts of the development of the organic laser materials have been directed toward organic solid-state lasers (OSSLs).[2–5] Noteworthy progress has been made in reducing the energy to begin laser emission where the gain of the laser medium equals the cavity loss. This performance is referred to as thresholds of amplified spontaneous emission (ASE) (E_{th}^{ASE}) and lasing (E_{th}^{laser}), and some organic materials are found to show very low thresholds close to 0.1 μJ cm^{-2}.[6–13] Also, the evolution of these advanced materials enabled the realization of continuous-wave (CW) lasers[14–18] and electrically pumped organic semiconducting laser diodes (OSLDs).[19] In such a situation, there has been increasing interest in the utilization of the long-lived triplet excitons in organic laser materials.[20–23]

The triplet harvesting in organic materials has been a critical issue in organic light-emitting diodes (OLEDs) because of the direct generation of triplet excitons via charge recombination under electrical excitation. Thus, the thermally activated delayed fluorescence (TADF) materials, which can upconvert triplet excitons to the single state through the reverse intersystem crossing (RISC), have been widely developed in a decade.[24–26] Recently, the RISC rates (k_{RISC}) have reached >10^7 s^{-1} upon deeper understanding of exciton dynamics, expanding possibilities of triplet utilization.[27,28] However, there are few examples of TADF materials showing lasing behaviour because the character of their excited states is generally charge transfer (CT) owing to the connection of the donor-acceptor structures, showing a rather slow radiative decay rate.[29–35] In addition, their thresholds are all significantly higher than 1 μJ cm^{-2},[36] which needs to be decreased to the level of fluorescent materials for practical applications.

The multiple-resonance effect (MRE) is an alternative strategy to achieve the TADF property, which was firstly demonstrated by DABNA derivatives with boron and nitrogen atoms.[37–42] Although the k_{RISC} of the MRE material was originally slow (~10^4 s^{-1}), it has also been improving.[43] Additional feature of MRE is a narrow full-width at half-maximum (FWHM) of less than 30 nm, which is advantageous to increasing optical gain. As a result, the DABNA derivative (DABNA-2, the inset in Fig. 1) showed the lowest E_{th}^{ASE} of close to 1 μJ cm^{-2} in TADF materials.[44] However, their potential has not been fully elucidated. In general, laser devices with optical resonators can further decrease the thresholds. For example, the E_{th}^{laser} of the fluorescent material could be reduced by one-third or less compared to E_{th}^{ASE}.[17] Therefore, the TADF materials should still have a chance to show promising thresholds as low as the fluorescent materials.

The properties of DABNA derivatives, including ASE behaviour, were characterized in doped films with a low concentration of less than 6 wt% because of strong concentration quenching.[45] However, both fluorescent CW laser and OSLD were realized in higher concentrations (>20

[a] Center for Organic Photonics and Electronics Research (OPERA), Kyushu University, Fukuoka 819-0395, Japan, E-mail: mamada@opera.kyushu-u.ac.jp; adachi@cstf.kyushu-u.ac.jp
[b] International Institute for Carbon Neutral Energy Research (WPI-I2CNER), Kyushu University, Nishi, Fukuoka 819-0395, Japan
[c] Department of Chemistry, Graduate School of Science and Technology, Kwansei Gakuin University, 2-1 Gakuen, Sanda, Hyogo 669–1337, Japan
[d] Department of Chemistry, Graduate School of Science, Kyoto University, Sakyo-ku, Kyoto 606-8502, Japan

† Electronic supplementary information (ESI) available: Synthesis, ASE, transient PL and stability data. For ESI, see DOI: 10.1039/

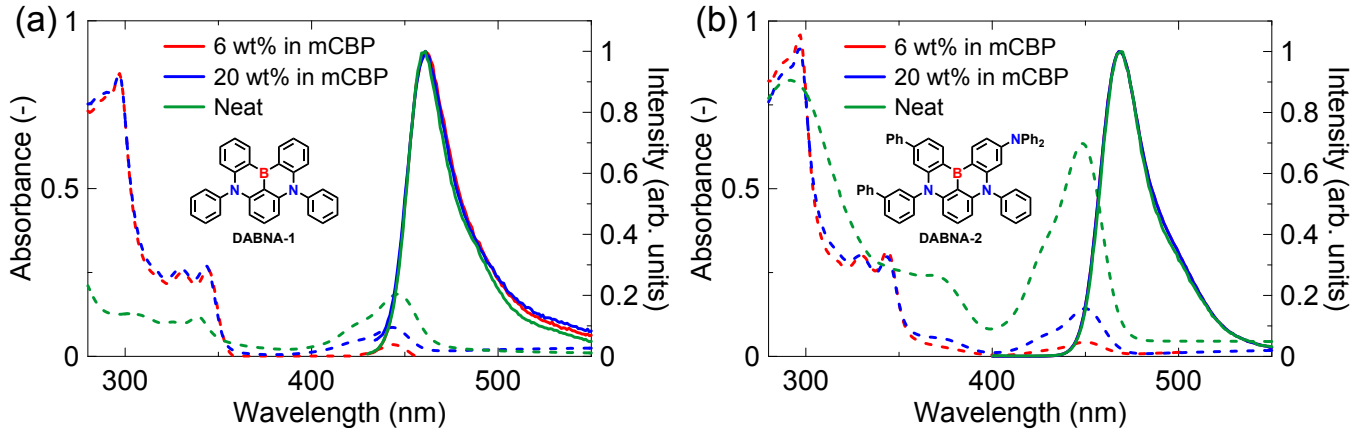

Fig. 1. UV-Vis absorption (dashed lines) and emission (solid lines) spectra for (a) DABNA-1 and (b) DABNA-2 in blend films of mCBP and neat films.

wt%) because of the issues of input light harvesting or charge carrier transporting. Thus, the photophysical properties of DABNA derivatives in aggregated/condensed forms should also be investigated.

In this work, we demonstrated a low E_{th}^{laser} from a TADF compound. In addition, DABNA derivatives are found to show ASE even in neat films despite very low photoluminescence (PL) quantum yield (Φ) by the serious concentration quenching. In order to suppress the concentration quenching, the blend films of two DABNA derivatives were fabricated, and lower thresholds compared to those in the sole DABNA system were achieved. Although these results using short pulse excitation and slow RISC materials include the negligible contribution of triplet excitons,[21] the very low E_{th} values comparable to those for fluorescent materials support the possibility of CW lasers and OSLDs using triplet excitons.

2. Experimental

General

Commercially available materials were used as received from the suppliers. Details of instruments and physical measurements are given in Table S1.

Materials synthesis and characterization

DABNA-1 and DABNA-2 were synthesized according to the reported methods.[37] DABNA-NP was prepared by modifying the literature (Methods S1).[40]

Film sample preparation

Thin films were fabricated on clean quartz substrates for optical measurements and on Si substrates with 1000 nm thick SiO_2 for ASE measurements. The substrates were cleaned with Cica clean, H_2O, acetone, and isopropanol, and then treated with UV/ozone to remove adsorbed organic species before deposition. Films were prepared by thermal evaporation at a pressure lower than 7×10^{-4} Pa. The deposition rates were 0.01 nm s^{-1} for the guest and 0.16 nm s^{-1} for the host for 6 wt% doped films.

ASE measurements

ASE properties of the thin films were characterized by optically pumping with a randomly polarized nitrogen gas laser (KEN2020, Usho Optical Systems Co., Ltd.) at an excitation wavelength of 337 nm with a 0.8 ns pulse (operating frequency of 20 Hz). The input laser beam was focused into a stripe with dimensions of ca. 0.6 cm × 0.1 cm using a cylindrical lens. Neutral density filters were used to adjust excitation intensity. ASE measurements were performed under a nitrogen atmosphere to prevent degradation. Output light emission from the edge of the sample was collected into an optical fibre connected to a spectrometer (Hamamatsu Photonics PMA-12). ASE thresholds were identified from the plot of output versus input intensity. Reproducibility was confirmed by measuring several different samples.

Distributed feedback (DFB) fabrication

The grating structure was fabricated according to the literature.[17] The SiO_2 surfaces were treated with hexamethyldisilazane (HMDS) by spin-coating at 200 rpm for 5 s and 4000 rpm for 15 s, and annealed at 120°C for 2 min. A resist layer was spin-coated at 4000 rpm for 30 s from a ZEP520A-7:ZEP-A solution (ZEON Co.) and baked at 180 °C for 4 min. ESPACER (Showa Denko K.K.) was spin-coated at 300 rpm for 5 s and 2000 rpm for 30 s. Electron beam lithography was performed to draw grating patterns using a JBX-5500SC system (JEOL) with an optimized dose of 0.1 nC cm^{-2}. The substrate was immersed in pure water for 1 min, and the patterns were developed in a developer ZED-N50 solution (ZEON Co.) at room temperature. The substrate was sonicated in isopropanol and annealed at 110 °C for 4 min. The substrate was plasma-etched with CHF_3 using an EIS-200ERT etching system (Elionix). The resist layer was entirely removed by washing with dimethylacetamide and treated with UV/ozone.

Laser measurements

After the deposition of an organic layer on the DFB substrate, CYCTOP (Asahi Glass Co. Ltd.) was spin-coated at 1000 rpm for 30 s, followed by sealing with sapphire lids on top of the laser devices, and dried in a vacuum overnight. The laser properties of the thin films were characterized by optically pumping with a randomly polarized nitrogen gas laser (KEN2020, Usho Optical Systems Co., Ltd.). The input laser beam was focused into a

Table 1. Photophysical and amplified spontaneous emission (ASE) properties of DABNA-1 and DABNA-2 in blend and neat films

Compound	Condition	λ_{PL} [nm]	Φ_{PL} [-][a]	τ [ns]	k_r / 10^8 [s^{-1}]	E_{th}^{ASE} [μJ cm^{-2}][b]	λ_{ASE} [nm]
DABNA-1	6 wt% in mCBP	461	85	8.3	1.0	3.3	479
	20 wt% in mCBP	461	62	6.6	0.94	8.8	481
	Neat	461	9	5.7 (2.5, 7.2)	0.16	18.4	493
DABNA-2	6 wt% in mCBP	468	89	6.0	1.5	2.1	494
	20 wt% in mCBP	468	61	5.4	1.1	4.3	497
	Neat	469	13	5.6 (1.3, 8.5)	0.23	12.7	500

[a] Absolute PL quantum yield evaluated using an integrating sphere. [b] Values obtained for 100 nm thick films.

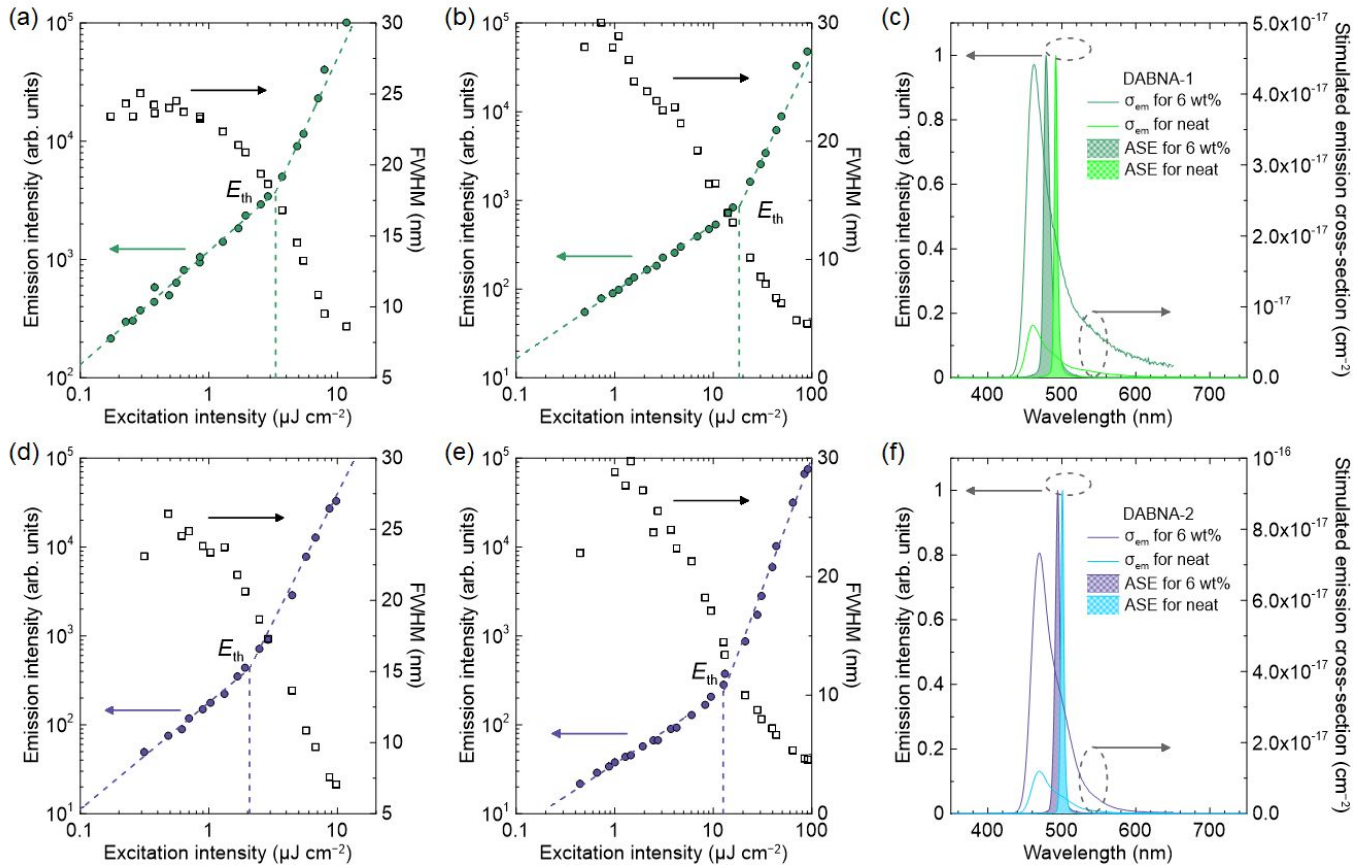

Fig. 2. PL intensity and FWHM values from edge of the 100-nm-thick films of (a) 6 wt%-DABNA-1 doped mCBP, (b) DABNA-1 neat, (d) 6 wt%-DABNA-2 doped mCBP, and (e) DABNA-2 neat. The stimulated cross-section spectra and PL spectra above the amplified spontaneous emission (ASE) threshold for the films of (c) DABNA-1 and (f) DABNA-2

circle with dimensions of ca. 0.1 cm × 0.1 cm. The excitation light was incident upon the devices at around 40° with respect to the normal to the device plane. The emitted light was collected normal to the device surface with an optical fibre connected to a multichannel spectrometer (PMA-50, Hamamatsu Photonics). Neutral density filters were used to adjust excitation intensity.

3. Results and discussion

ASE and Laser from sole DABNA system

The ASE properties of DABNA-1 and DABNA-2 were investigated in doped films with a 3,3'-di(9*H*-carbazol-9-yl)-1,1'-biphenyl (mCBP) host.[44] Thus, we fabricated the blend films using mCBP with 6 wt%- and 20 wt%-DABNA concentrations and the neat films. The UV-Vis absorption and PL spectra for these films with 100-nm-thickness are shown in Fig. 1. The lowest-energy absorption bands (0-0) for DABNA-1 and DABNA-2 neat films are nearly the same (446 nm and 448 nm, respectively), while the extinction coefficient of DABNA-2 is apparently high. Interestingly, the PL maxima are not dependent on the concentrations for both compounds. However, the Φ was significantly decreased in the higher concentrations (Table 1). The radiative rate constants (k_r) of DABNA-2 calculated from Φ and fluorescence lifetime (τ) are higher than those of DABNA-1 in agreement with the oscillator strength difference in absorption spectra. Although DABNA-2 has some substituents

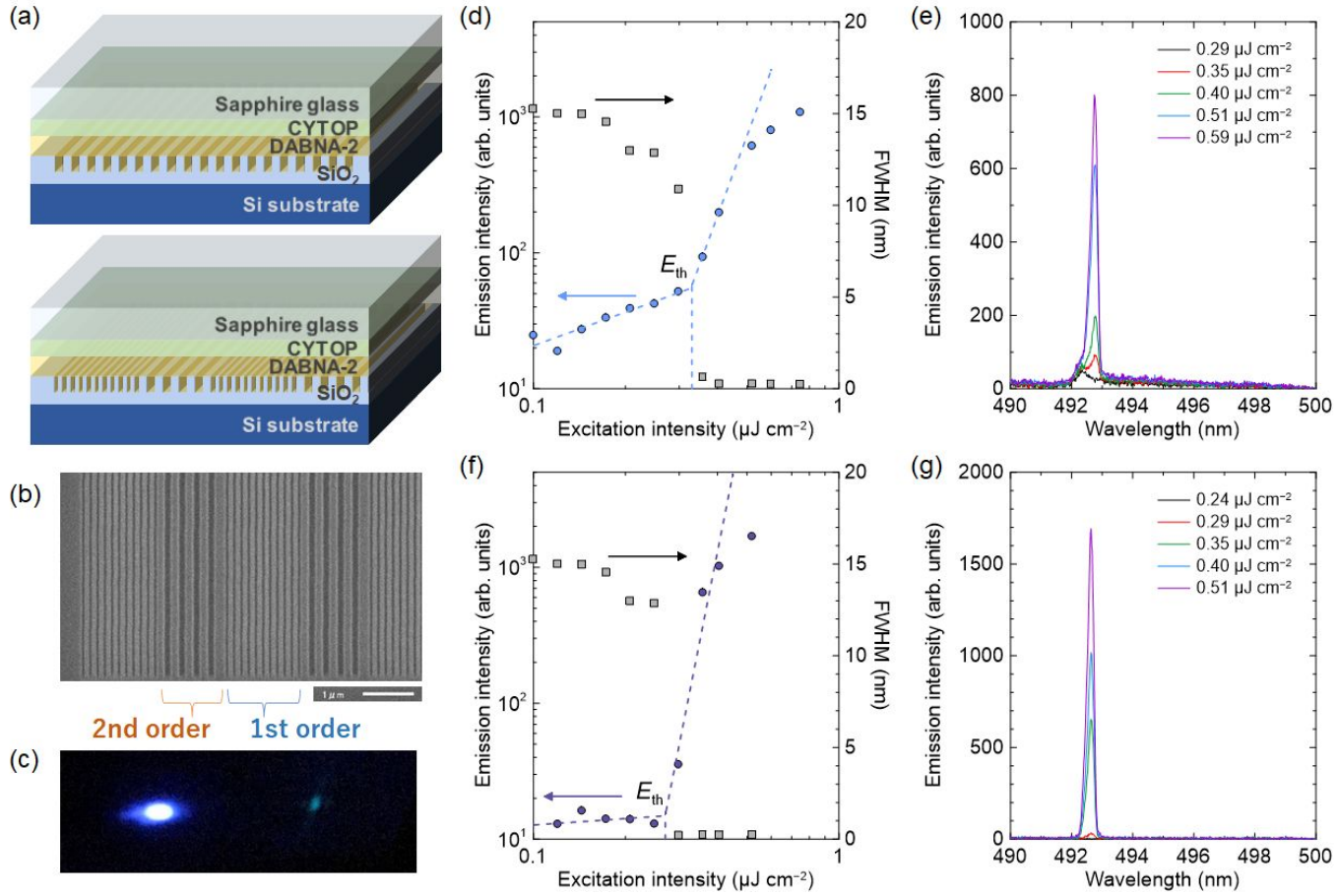

Fig. 3. Laser properties of 6 wt% DABNA-2 doped film of mCBP with 100 nm thickness. (a) Schematic image of the second-order DFB (top) and mixed-order DFB (bottom). (b) SEM image of the mixed-order DFB structure. (c) Laser emission from the surface of the DFB device. PL intensity and FWHM values for (d) second-order DFB and (f) mixed-order DFB. The PL spectra at different excitation energies for (e) second-order DFB and (g) mixed-order DFB.

on the DABNA-1 structure which seem to contribute to preventing intermolecular interactions between the core structures, no clear difference in the concentration quenching between two DABNA derivatives was observed. The k_r values of the 20 wt% doped films are close to 1×10^8 s^{-1} for both DABNA derivatives, indicating the high potential of DABNA at higher doping concentration for use in laser.

The light amplification behaviour of DABNA derivatives was evaluated by using a nitrogen gas laser. The E_{th}^{ASE} values (Table 1) were determined from a change in slope in output emission intensity as a function of excitation intensity as shown in Fig. 2. The optimized thickness was 100 nm in the previous report,[44] which was confirmed by fabricating thicker films with 200 nm (Fig. S1 and Table S2). The higher doping concentration of 20 wt% resulted in a slight increase of the E_{th}^{ASE}, and the trend agrees well with the decreased Φ and k_r. Interestingly, the neat films for DABNA-1 and DABNA-2 showed the ASE as clearly confirmed by the narrowed spectra (Fig. 2c and 2f). The E_{th}^{ASE} values in the neat films were increased relative to those for the doped films, while these are much lower than those expected from the small values of stimulated emission cross-section (σ_{em}) (Methods S2). The emission decay for the neat films in time-resolved PL measurement includes two components and the faster decay might contribute to the light amplification. Here, we note that the ASE maxima corresponding to 0-1 transition were slightly redshifted with increasing the concentrations. This might be due to the increase of self-absorption, but also a small change in the vibrational level of the ground state by the aggregation since the shift for DABNA-1 (14 nm) is relatively larger than that for DABNA-2 (6 nm). Indeed, the lowest absorption bands slightly shifted (~2 nm) and broadened with increasing concentration, indicating aggregation-caused effect (Fig. S2). Overall, DABNA-2 showed better ASE properties than DABNA-1 in any condition.

The lasing characteristics of DABNA-2 were investigated using distributed feedback (DFB) resonators. Firstly, the grating period (Λ) was calculated by the Bragg condition $m\lambda_{Bragg} = 2n_{eff}\Lambda_m$, where m is the order of diffraction, λ_{Bragg} is the Bragg wavelength, and n_{eff} is the effective refractive index of the waveguide.[4,46] The first-order (m = 1) provides in-plane feedback by first-order diffraction, resulting in an edge-emitting laser. The laser beam in second-order (m = 2) is emitted from the surface of the film perpendicular to the substrate plane via first-order Bragg scattering where the optical feedback is provided by in-plane second-order diffraction. We selected second-order DFB because the surface-emitting laser is preferable for future OSL applications. In addition, the larger grating period is technically easy in fabrication, resulting in

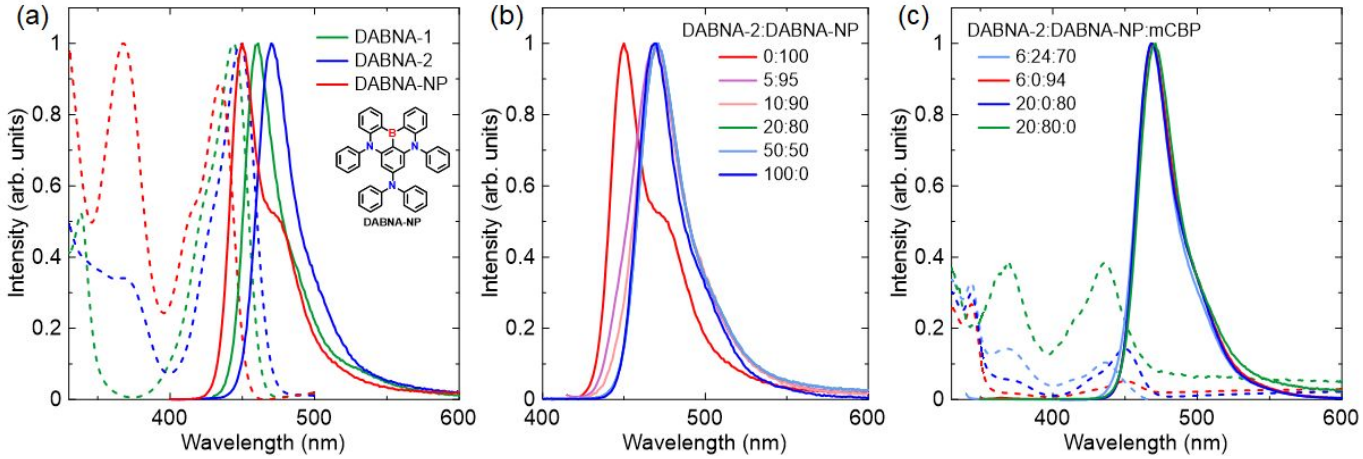

Fig. 4. UV-Vis absorption (dashed lines) and emission (solid lines) spectra for (a) the neat films of DABNA derivatives, (b) the blend films of DABNA-2 and DABNA-NP, and (c) the blend films of DABNA-2:DABNA-NP:mCBP.

Table 2. Photophysical and ASE properties of the blend films of DABNA-2:DABNA-NP:mCBP

DABNA-2 [wt%]	DABNA-NP [wt%]	mCBP [wt%]	λ_{PL} [nm]	Φ_{PL} [-][a]	τ [ns]	k_r / 10^8 [s^{-1}]	E_{th}^{ASE} [μJ cm^{-2}][b]	λ_{ASE} [nm]
0	100	0	450	9	4.6 (1.4, 6.1)	0.20	-	-
5	95	0	469	15	3.9	0.48	-	-
10	90	0	471	19	3.3	0.45	-	-
20	80	0	471	24	5.4	0.44	9.8	491
50	50	0	471	12	5.9	0.20	-	-
6	24	70	469	78	6.1	1.3	3.3	495

[a] Absolute PL quantum yield evaluated using an integrating sphere. [b] Values obtained for 100 nm thick films

higher quality of the grating. However, the E_{th}^{laser} in the first-order is normally lower than that in the second-order. Thus, the mixed-order DFB with efficient in-plane feedback and surface outcoupling was also fabricated (Fig. 3). The grating periods were calculated to be 160 (Λ_1) and 320 nm (Λ_2). After the deposition of a 100-nm thick layer of 6 wt% DABNA-2 doped mCBP, the transparent fluoropolymer CYTOP and sapphire glass were assembled on top of the DABNA layer for the passivation. The DFB devices showed a clear laser beam at low excitation intensity. The peak wavelength of ca. 493 nm is close to the ASE wavelength, indicating that the grating periods were optimal architectures. The strong surface emission and the reduction of FWHM to <0.30 nm prove lasing. The E_{th}^{laser} of 0.35 μJ cm^{-2} for the second-order DFB device and 0.27 μJ cm^{-2} for the mixed-order DFB device were obtained. These values are considerably decreased from E_{th}^{ASE}, probably attributed to reducing inefficient primary self-reabsorption at 0-0 transition with the optical feedback. These thresholds are surely the best in TADF materials and comparable to those in excellent fluorescent materials.

Mixed DABNA films

The small stokes shift for DABNA caused strong self-absorption, which might lead to a decrease of the Φ. Because the doped films showed high Φ, we came up with the utilization of DABNA as the host for different DABNA emitters. However, the spectral differences between DABNA-1 and DABNA-2 are very small. Therefore, DABNA-NP (the inset in Fig. 4) with the additional functional group on the DABNA-1 structure was selected.[47] The PL spectrum of DABNA-NP was blueshifted, resulting in a large overlap with the absorption of DABNA-2 (Fig. 4a). Note that DABNA-NP shows slightly poor photophysical properties than DABNA-1 (Φ = 67%, τ = 6.1 ns, E_{th}^{ASE} = 16 μJ cm^{-2} for 6 wt% DABNA-NP doped mCBP film, Fig. S3), indicating that it is insignificant as the emitter. The PL spectra of the binary blended DABNA-2:DABNA-NP films were almost the same as that of DABNA-2 neat film when the doping concentration increased to 20 wt%, indicating efficient energy transfer possible (Fig. 4b). In addition, the Φ values were increased up to almost double of the neat film of DABNA-2 with the increase of the doping concentration of DABNA-2 to 20 wt% (Table 2). The higher concentration of 50 wt% resembles the neat films. Thus, the ratio of 1:4 of DABNA-2:DABNA-NP is considered to be the optimal condition. This design can be further extended to doped films in mCBP. The ternary blend film of DABNA-2:DABNA-NP:mCBP with the concentrations of 6:24:70 wt% with 30 wt% total DABNA ratio shows a high Φ of 78% and k_r of 1.3 × 10^8 s^{-1}, which are better than a 20 wt% DABNA-2 doped film of mCBP. The light harvesting ability at 350–440 nm for the ternary system was increased compared to DABNA-2 doped films in mCBP (Fig. 4c). Thus, this strategy is useful for increasing the concentration while improving the photophysical properties. It is noteworthy that the delayed fluorescence was clearly observed with the energy transfer from DABNA-NP to DABNA-2 (Fig. S4). This result also suggests that the MRE materials have

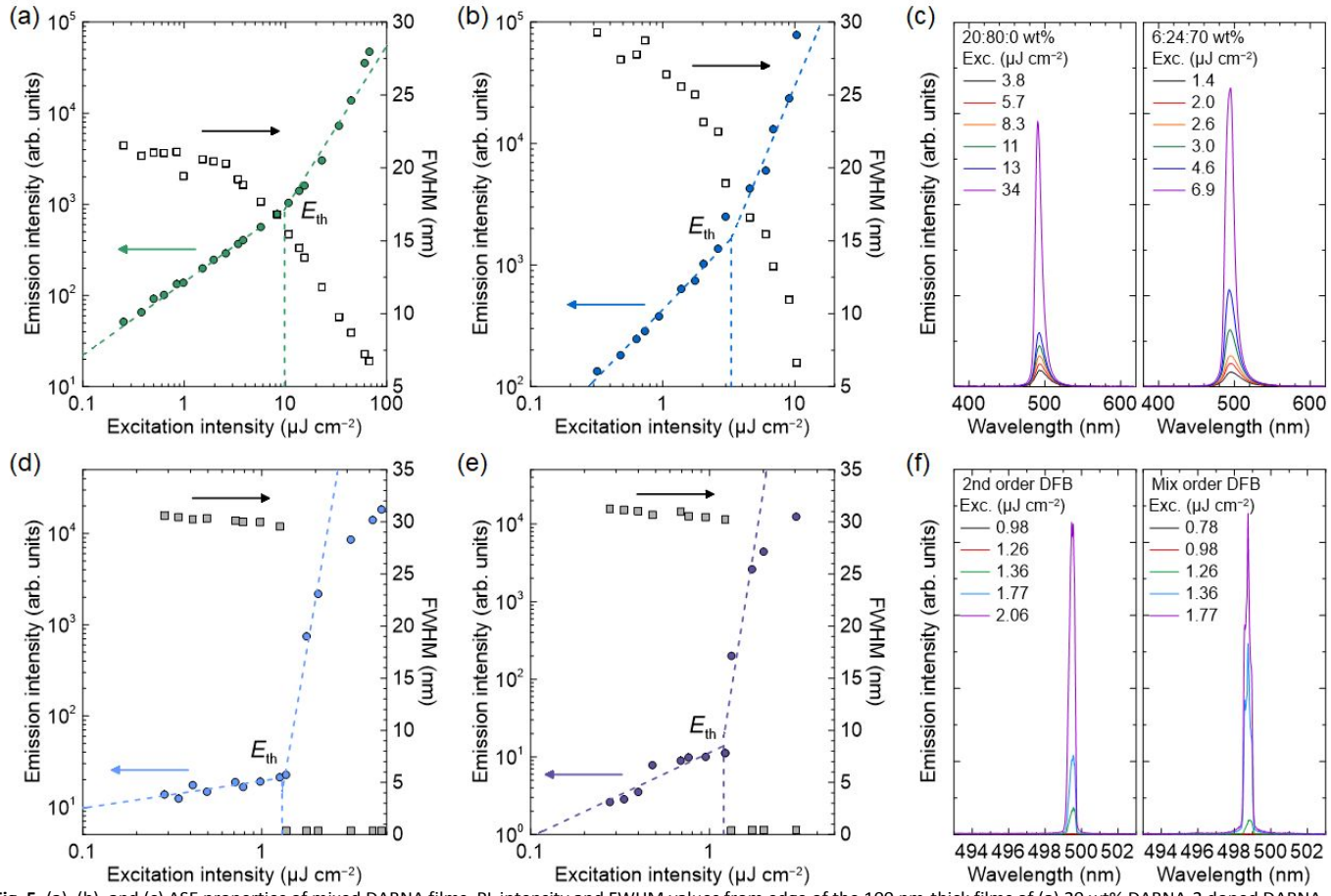

Fig. 5. (a), (b), and (c) ASE properties of mixed DABNA films. PL intensity and FWHM values from edge of the 100 nm-thick films of (a) 20 wt% DABNA-2 doped DABNA-NP and (b) 6 wt% DABNA-2 and 24 wt% DABNA-NP doped mCBP. (c) The PL spectra at different excitation energies for the ASE measurements. (d), (e), and (f) Laser properties of 6 wt% DABNA-2 and 24 wt% DABNA-NP doped films of mCBP with 100 nm thickness. PL intensity and FWHM values for (d) second-order DFB and (e) mixed-order DFB. (f) The PL spectra at different excitation energies.

potential to be used as an assistant dopant in the hyperfluorescence OLED.

The light amplification abilities of mixed DABNA films were evaluated as shown in Fig. 5. The E_{th}^{ASE} values of binary and ternary films were 9.8 and 3.3 μJ cm^{-2}, respectively. These were improved from those for the DABNA-2 neat (12.7 μJ cm^{-2}) and 20 wt% DABNA-2 doped mCBP films (4.3 μJ cm^{-2}), respectively. The DFB laser devices for the ternary film were also fabricated as the same as above. The clear laser peak was observed in both the second-order and the mixed-order DFB devices with the E_{th}^{laser} values of 1.3 and 1.2 μJ cm^{-2}, respectively. The peak maxima of the lasing wavelength were ca. 499 nm with the FWHM of <0.4 nm, which is slightly shifted from the peak of the ASE spectrum, probably due to the slight change of n_{eff} by incorporating DABNA-NP. Thus, these thresholds may be able to slightly reduce further, although these are already better than those for other TADF molecules.

4. Conclusions

We successfully evaluated the laser properties of the TADF emitter DABNA-2. The E_{th}^{laser} could be decreased to 0.27 μJ cm^{-2} in the mixed-order DFB device, which is comparable to those for the excellent fluorescent materials. Thus, as the next step, by upconverting triplets into singlets in DABNAs, we can expect realizing the CW and electrically pumped lasing with lower threshold. In particular, the TADF process should be able to significantly contribute under electrical excitation with direct triplet generation and a relatively long voltage pulse operation.[19,48] However, the stability of the laser device should be improved in the future work, probably a high-quality DFB structure is necessary (Fig. S5). In addition, the design of fast k_{RISC} materials needs to be optimized for laser materials.

Interestingly, the neat films of DABNA derivatives showed light amplification, although they had a strong concentration quenching. To improve the optical properties in the aggregated state, the blend films of DABNA-2 and DABNA-NP were also fabricated. DABNA-NP successfully worked as an assist dopant, realizing efficient energy transfer from DABNA-NP to DABNA-2 and improved Φ. These findings open up great prospects for TADF materials utilizing in laser applications.

Conflicts of interest

There are no conflicts to declare.

Acknowledgements

This work was financially supported by JSPS KAKENHI Grant Number 20K21227 and 21H05401, JST CREST Grant Number JPMJCR22B3, and JSPS Core-to-Core Program (JPJSCCA20180005).

Notes and references

1 F. P. Schäfer, W. Schmidt and J. Volze, Organic dye solution laser, *Appl. Phys. Lett.*, 1966, **9**, 306–309.
2 N. Tessler, G. J. Denton and R. H. Friend, Lasing from conjugated-polymer microcavities, *Nature*, 1996, **382**, 695–697.
3 F. Hide, M. A. DiazGarcia, B. J. Schwartz, M. R. Andersson, Q. B. Pei and A. J. Heeger, Semiconducting polymers: a new class of solid-state laser materials, *Science*, 1996, **273**, 1833–1836.
4 I. D. W. Samuel and G. A. Turnbull, Organic semiconductor lasers, *Chem. Rev.*, 2007, **107**, 1272–1295.
5 A. J. C. Kuehne and M. C. Gather, Organic lasers: recent developments on materials, device geometries, and fabrication techniques, *Chem. Rev.*, 2016, **116**, 12823–12864.
6 T. W. Lee, O. O. Park, D. H. Choi, H. N. Cho and Y. C. Kim, *Appl. Phys. Lett.*, Low-threshold blue amplified spontaneous emission in a statistical copolymer and its blend, 2002, **81**, 424–426.
7 A. Rose, Z. G. Zhu, C. F. Madigan, T. M. Swager and V. Bulovic, Sensitivity gains in chemosensing by lasing action in organic polymers, *Nature*, 2005, **434**, 876–879.
8 H. Nakanotani, S. Akiyama, D. Ohnishi, M. Moriwake, M. Yahiro, T. Yoshihara, S. Tobita and C. Adachi, Extremely low-threshold amplified spontaneous emission of 9,9'-spirobifluorene derivatives and electroluminescence from field-effect transistor structure, *Adv. Funct. Mater.*, 2007, **17**, 2328–2335.
9 C. Karnutsch, C. Pflumm, G. Heliotis, J. C. deMello, D. D. C. Bradley, J. Wang, T. Weimann, V. Haug, C. Gärtner and U. Lemmer, Improved organic semiconductor lasers based on a mixed-order distributed feedback resonator design, *Appl. Phys. Lett*., 2007, **90**, 131104.
10 R. Xia, W.-Y. Lai, P. A. Levermore, W. Huang and D. D. C. Bradley, Low-threshold distributed-feedback lasers based on pyrene-cored starburst molecules with 1,3,6,8-attached oligo(9,9-dialkylfluorene) arms, *Adv. Funct. Mater.* 2009, **19**, 2844–2850.
11 D.-H. Kim, A. S. D. Sandanayaka, L. Zhao, D. Pitrat, J. C. Mulatier, T. Matsushima, C. Andraud, J.-C. Ribierre and C. Adachi, Extremely low amplified spontaneous emission threshold and blue electroluminescence from a spin-coated octafluorene neat film, *Appl. Phys. Lett.*, 2017, **110**, 023303.
12 M. Mamada, T. Fukunaga, F. Bencheikh, A. S. D. Sandanayaka and C. Adachi, Low amplified spontaneous emission threshold from organic dyes based on bis-stilbene, *Adv. Funct. Mater.*, 2018, **28**, 1802130.
13 Y, Oyama, M. Mamada, A. Shukla, E. G. Moore, S.-C. Lo, E. B. Namdas and C. Adachi, Design strategy for robust organic semiconductor laser dyes, *ACS Mater. Lett.*, 2020, **2**, 161−167.
14 R. Bornemann, U. Lemmer and E. Thiel, Continuous-wave solid-state dye laser, *Opt. Lett.*, 2006, **31**, 1669–1671.
15 T. Rabe, K. Gerlach, T. Riedl, H.-H. Johannes, W. Kowalsky, J. Niederhofer, W. Gries, J. Wang, T. Weimann, P. Hinze, F. Galbrecht and U. Scherf, Quasi-continuous-wave operation of an organic thin-film distributed feedback laser, *Appl. Phys. Lett.*, 2006, **89**, 081115.
16 A. S. D. Sandanayaka, K. Yoshida, M. Inoue, C. Qin, K. Goushi, J.-C. Ribierre, T. Matsushima and C. Adachi, Quasi-continuous-wave organic thin-film distributed feedback laser, *Adv. Opt. Mater.*, 2016, **4**, 834–839.
17 A. S. D. Sandanayaka, T. Matsushima, F. Bencheikh, K. Yoshida, M. Inoue, T. Fujihara, K. Goushi, J.-C. Ribierre and C. Adachi, Toward continuous-wave operation of organic semiconductor lasers, *Sci. Adv.*, 2017, **3**, e1602570.
18 V. T. N. Mai, A. Shukla, A. M. C. Senevirathne, I. Allison, H. Lim, R. J. Lepage, S. K. M. McGregor, M. Wood, T. Matsushima, E. G. Moore, E. H. Krenske, A. S. D. Sandanayaka, C. Adachi, E. B. Namdas and S.-C. Lo, Lasing operation under long-pulse excitation in solution-processed organic gain medium: toward CW lasing in organic semiconductors, *Adv. Opt. Mater.*, 2020, **8**, 2001234.
19 A. S. D. Sandanayaka, T. Matsushima, F. Bencheikh, S. Terakawa, W. J. Potscavage, C. Qin, T. Fujihara, K. Goushi, J.-C. Ribierre and C. Adachi, Indication of current-injection lasing from an organic semiconductor, *Appl. Phys. Express*, 2019, **12**, 061010.
20 H. Nakanotani, T. Furukawa and C. Adachi, Light amplification in an organic solid-state film with the aid of triplet-to-singlet upconversion, *Adv. Opt. Mater.*, 2015, **3**, 1381.
21 A. Abe, K. Goushi, A. S. D. Sandanayaka, R. Komatsu, T. Fujihara, M. Mamada and C. Adachi, Numerical study of triplet dynamics in organic semiconductors aimed for the active utilization of triplets by TADF under continuous-wave lasing, *J. Phys. Chem. Lett.*, 2022, **13**, 1323–1329.
22 A. Shukla, S. K. M. McGregor, R. Wawrzinek, S. Saggar, E. G. Moore, S.-C. Lo and E. B. Namdas, Light amplification and efficient electroluminescence from a solution-processable diketopyrrolopyrrole derivative via triplet-to-singlet upconversion, *Adv. Funct. Mater.* 2021, **31**, 2009817.
23 A. Shukla, M. Hasan, G. Banappanavar, V. Ahmad, J. Sobus, E. G. Moore, D. Kabra, S.-C. Lo and E. B. Namdas, Controlling triplet–triplet upconversion and singlet-triplet annihilation in organic light-emitting diodes for injection lasing, *Commun. Mater.* 2022, **3**, 27.
24 H. Uoyama, K. Goushi, K Shizu, H. Numura and C. Adachi, Highly efficient organic light-emitting diodes from delayed fluorescence, *Nature*, 2012, **492**, 234–238.
25 G. Hong, X. Gan, C. Leonhardt, Z. Zhang, J. Seibert, J. M. Busch and S. Bräse, A brief history of OLEDs—emitter development and industry milestones, *Adv. Mater.*, 2021, **33**, 2005630.
26 H. Imahori, Y. Kobori and H. Kaji, Manipulation of charge-transfer states by molecular design: perspective from "dynamic exciton", *Acc. Mater. Res.* 2021, **2**, 501–514.
27 L.-S. Cui, A. J. Gillett, S.-F. Zhang, H. Ye, Y. Liu, X.-K. Chen, Z.-S. Lin, E. W. Evans, W. K. Myers, T. K. Ronson, H. Nakanotani, S. Reineke, J.-L. Bredas, C. Adachi and R. H. Friend, Fast spin-flip enables efficient and stable organic electroluminescence from charge-transfer states, *Nat. Photonics*, 2020, **14**, 636–642.
28 Y. Wada, H. Nakagawa, S. Matsumoto, Y. Wakisaka and H. Kaji, Organic light emitters exhibiting very fast reverse intersystem crossing, *Nat. Photonics*, 2020, **14**, 643–649.
29 S. Park, O.-H. Kwon, S. Kim, S. Park, M.-G. Choi, M. Cha, S. Y. Park and D.-J. Jang, Imidazole-based excited-state intramolecular proton-transfer materials: synthesis and amplified spontaneous emission from a large single crystal, *J. Am. Chem. Soc.*, 2005, **127**, 10070–10074.
30 S. Park, O.-H. Kwon, Y.-S. Lee, D.-J. Jang and S. Y. Park, Imidazole-based excited-state intramolecular proton-transfer (ESIPT) materials: observation of thermally activated delayed fluorescence (TDF), *J. Phys. Chem. A*, 2007, **111**, 9649–9653.
31 D.-H. Kim, A. D'Aléo, X.-K. Chen, A. D. S. Sandanayaka, D. Yao, L. Zhao, T. Komino, E. Zaborova, G. Canard, Y. Tsuchiya, E. Choi, J. W. Wu, F. Fages, J.-L. Brédas, J.-C. Ribierre and C. Adachi, High-efficiency electroluminescence and amplified spontaneous emission from a thermally activated delayed

fluorescent near-infrared emitter, *Nat. Photonics*, 2018, **12**, 98–104.

32 R. Aoki, R. Komatsu, K. Goushi, M. Mamada, S. Y. Ko, J. W. Wu, V. Placide, A. D'Aléo and C. Adachi, Realizing near-infrared laser dyes through a shift in excited-state absorption, *Adv. Opt. Mater.*, 2021, **9**, 2001947.

33 A. Khan, X. Tang, C. Zhong, Q. Wang, S. Yang, F. Kong, S. Yuan, A. S. D. Sandanayaka, C. Adachi, Z. Jiang and L. Liao, Intramolecular-locked high efficiency ultrapure violet-blue (CIE-y <0.046) thermally activated delayed fluorescence emitters exhibiting amplified spontaneous emission, *Adv. Funct. Mater.*, 2021, **31**, 2009488.

34 Y. Li, K. Wang, Q. Liao, L. Fu, C. Gu, Z. Yu and H. Fu, Tunable triplet-mediated multicolor lasing from nondoped organic TADF microcrystals, *Nano Lett.*, 2021, **21**, 3287–3294.

35 T. Zhang, Z. Zhou, X. Liu, K. Wang, Y. Fan, C. Zhang, J. Yao, Y. Yan and Y. S. Zhao, Thermally activated lasing in organic microcrystals toward laser displays, *J. Am. Chem. Soc.*, 2021, **143**, 20249–20255.

36 C.-C. Yan, X.-D. Wang and L.-S. Liao, Thermally activated delayed fluorescent gain materials: harvesting triplet excitons for lasing, *Adv. Sci.*, 2022, **9**, 2200525.

37 T. Hatakeyama, K. Shiren, K. Nakajima, S. Nomura, S. Nakatsuka, K. Kinoshita, J. Ni, Y. Ono and T. Ikuta, Ultrapure blue thermally activated delayed fluorescence molecules: effi cient HOMO–LUMO separation by the multiple resonance effect, *Adv. Mater.*, 2016, **28**, 2777–2781.

38 K. Matsui, S. Oda, K. Yoshiura, K. Nakajima, N. Yasuda and T Hatakeyama, One-shot multiple borylation toward BN-doped nanographenes, *J. Am. Chem. Soc.* 2018, **140**, 1195–1198.

39 Y. Kondo, K. Yoshiura, S. Kitera, H. Nishi, S. Oda, H. Gotoh, Y. Sasada, M. Yanai and T. Hatakeyama, Narrowband deep-blue organic light-emitting diode featuring an organoboron-based emitter, *Nat. Photonics*, 2019, **13**, 678–682.

40 S. Oda, W. Kumano, T. Hama, R. Kawasumi, K. Yoshiura and T. Hatakeyama, Carbazole-based DABNA analogues as highly efficient thermally activated delayed fluorescence materials for narrowband organic light-emitting diodes, *Angew. Chem. Int. Ed.* 2021, **60**, 2882–2886.

41 S. Oda and T. Hatakeyama, Development of one-shot/one-pot borylation reactions toward organoboron-based materials, *Bull. Chem. Soc. Jpn.*, 2021, **94**, 950–960.

42 S. M. Suresh, D. Hall, D. Beljonne, Y. Olivier and E. Zysman-Colman, Multiresonant thermally activated delayed fluorescence emitters based on heteroatom-doped nanographenes: recent advances and prospects for organic light-emitting diodes, *Adv. Funct. Mater.*, 2020, **30**, 1908677.

43 Y. X. Hu, J. Miao, T. Hua, Z. Huang, Y. Qi, Y. Zou, Y. Qiu, H. Xia, H. Liu, X. Cao and C. Yang, Efficient selenium-integrated TADF OLEDs with reduced roll-off, *Nat. Photonics*, 2022, **16**, 803–810.

44 H. Nakanotani, T. Furukawa, T. Hosokai, T. Hatakeyama and C. Adachi, Light amplification in molecules exhibiting thermally activated delayed fluorescence, *Adv. Opt. Mater.*, 2017, **5**, 1700051.

45 S. H. Han, J. H. Jeong, J. W. Yoo and J. Y. Lee, Ideal blue thermally activated delayed fluorescence emission assisted by a thermally activated delayed fluorescence assistant dopant through a fast reverse intersystem crossing mediated cascade energy transfer process, *J. Mater. Chem. C*, 2019, **7**, 3082–3089.

46 S. Chenais and S. Forget, Recent advances in solid-state organic lasers, *Polym. Int.*, 2012, **61**, 390–406.

47 Y. Wang, Y. Duan, R. Guo, S. Ye, K. Di, W. Zhang, S. Zhuang and L. Wang, A periphery cladding strategy to improve the performance of narrowband emitters, achieving deep-blue OLEDs with CIEy < 0.08 and external quantum efficiency approaching 20%, *Org. Electron.*, 2021, **97**, 106275.

48 V. Ahmad, J. Sobus, M. Greenberg, A. Shukla, B. Philippa, A. Pivrikas, G. Vamvounis, R. White, S.-C. Lo and E. B. Namdas, Charge and exciton dynamics of OLEDs under high voltage nanosecond pulse: towards injection lasing, *Nat. Commun.*, 2020, **11**, 4310.